

Electronic Supplementary Information for

Unravelling co-catalyst integration methods in Ti-based metal-organic gels for photocatalytic H₂ production

Maite Perfecto-Irigaray,^a Garikoitz Beobide,^{*a,b} Oscar Castillo,^{a,b} Michael G. Allan,^{c,d} Moritz F. Kühnel,^{*c,e} Antonio Luque,^{a,b} Harishchandra Singh,^f Ashok Kumar Yadav^g and Sonia Pérez-Yáñez^{a,b}

^a Department of Organic and Inorganic Chemistry, University of the Basque Country, UPV/EHU, P.O. 644, Bilbao E-48080, Spain.

^b BCMaterials, Basque Center for Materials, Applications and Nanostructures, UPV/EHU Science Park, Leioa 48940, Spain.

^c Department of Chemistry, Faculty of Science and Engineering, Swansea University, Singleton Park, SA2 8PP Swansea, Wales.

^d North Campus Research Complex, University of Michigan, Ann Arbor, MI, 48109, United States of America

^e Institute of Chemistry, University of Hohenheim, 70593 Stuttgart, Germany.

^f Nano and Molecular Systems Research Unit, University of Oulu, Oulu FIN-90014, Finland.

^g Synchrotron SOLEIL, Beamline SIRIUS, Saint-Aubin, F-91192, Gif sur Yvette, France

S1. REAGENTS AND SOLVENTS.....	2
S2. PROCESSING OF MOGs.....	3
S3. PROTON NUCLEAR MAGNETIC RESONANCE (¹ H-NMR).....	4
S4. THERMOGRAVIMETRIC ANALYSIS (TGA).....	7
S5. DEFECTIVE FORMULA ESTIMATION	9
S6. FOURIER-TRANSFORM INFRARED SPECTROSCOPY (FTIR).....	10
S7. SCANNING ELECTRON MICROSCOPY (SEM).....	11
S8. SYNCHROTRON X-RAY ABSORPTION SPECTROSCOPY.....	12
S9. UV-Vis DIFFUSE REFLECTANCE SPECTROSCOPY (DRS) AND BAND GAP CALCULATIONS.....	14
S10. LIGHT-DRIVEN HYDROGEN EVOLUTION REACTION (HER) EXPERIMENTS	16

S1. REAGENTS AND SOLVENTS

Reagents and solvents employed during synthetic and catalytic procedures were used as commercially obtained. Table S1 shows them sorted alphabetically, along with some data of interest and the role played in the experimental process they were involved.

Table S1 Reagents employed in the experimental methods.^a

Reagent	Formula	Commercial House	Assay (%)	ρ (g·cm ⁻³) (20 °C)	MW (g·mol ⁻¹)	Process
2-aminobenzene-1,4-dicarboxylic acid / 2-aminoterephthalic acid	C ₈ H ₇ NO ₄ (<i>H₂NH₂BDC</i>)	Sigma Aldrich	99	–	181.15	Organic ligand
Absolute ethanol	CH ₃ CH ₂ OH / C ₂ H ₅ OH (<i>EtOH</i>)	Scharlab	ACS	0.789	46.07	Synthesis and cleaning solvent
Benzene-1,4-dicarboxylic acid / terephthalic acid	C ₈ H ₆ O ₄ (<i>H₂BDC</i>)	Sigma Aldrich	98	–	166.13	Organic ligand
Butan-2-ol	CH ₃ CH ₂ CH(OH)CH ₃	Alfa Aesar	99+	0.808	74.12	Synthesis and cleaning solvent
Copper(II) nitrate hemi(pentahydrate)	Cu(NO ₃) ₂ ·2.5H ₂ O	Sigma Aldrich	98	–	232.59	Copper(II) source
Deionised water	DI H ₂ O	–	–	0.998	18.01	Cleaning solvent
Deuterium oxide / deuterated water	D ₂ O	Sigma Aldrich	99.9	1.11	20.03	¹ H-NMR digestions
Hexachloroplatinic(IV) acid hydrate	H ₂ PtCl ₆ ·xH ₂ O	Sigma Aldrich	99.9	–	409.81 (anhydrous)	Platinum(IV) source
Hydrochloric acid	HCl	Labkem	35-38 (w/w) AGR	1.12	36.46	Acidification
N,N-dimethylformamide	(CH ₃) ₂ NCHO (<i>DMF</i>)	Labkem	99.9	0.95	73.09	Synthesis and cleaning solvent
Pottasium bromide	KBr	Sigma Aldrich	99	–	119.00	FTIR pellets preparation
Sodium hydroxyde	NaOH	Sigma Aldrich	98	–	40.00	Basification and digestion
Titanium(IV) n-butoxide	Ti(CH ₃ CH ₂ CH ₂ CH ₂ O) ₄	Thermo Scientific	99+	0.998	340.36	Titanium(IV) source
trans-butenedioic acid / fumaric acid	HO ₂ CCH=CHCO ₂ H	Sigma Aldrich	99	–	116.07	¹ H-NMR internal standard
Triethanolamine	(HOCH ₂ CH ₂) ₃ N	Sigma Aldrich	98	–	149.19	Electron donor

^a ρ : density, MW: molecular weight, FTIR: Fourier-transform infrared, ¹H-NMR: proton nuclear magnetic resonance.

S2. PROCESSING OF MOGs

Prior to the characterization of the materials, synthesised gels were washed by solvent exchange to remove excess of reagent. Thereafter, for chemical characterization, N₂ physisorption measurements and SEM analysis the solvent was removed by evaporation or supercritical drying. Alternatively, hydrogels were prepared for cryoTEM analysis and HER experiments. As a representative examples, Fig. S1 shows the appearance of prepared A100 MOG through manipulating, washing, and drying processes, illustrating the different types of materials employed in characterization and HER experiments.

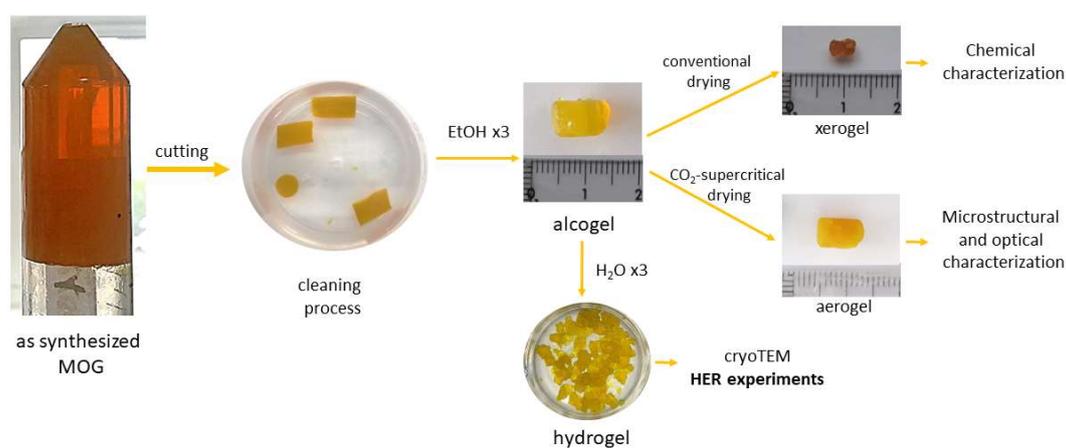


Fig. S1 Cleaning, drying and characterization scheme followed for MOGs along the study.

S3. PROTON NUCLEAR MAGNETIC RESONANCE ($^1\text{H-NMR}$)

To proceed with $^1\text{H-NMR}$ spectrum (500 MHz), 50 mg of each dry MOG (B100, B50A50 and A100) was digested in 2 mL of a 1 M NaOH solution (in deuterated water, D_2O). The digestion was prolonged for 1 h, after which fumaric acid was added as an internal standard (20 mg), and the solid residue was filtered off. The NMR spectrum was then taken on the liquid fraction.

Fig. S2. shows the label assignment of the species identified in the NMR spectra. In all of them, the singlet at 6.45 ppm is related to the two vinylic ^1H -atoms of fumaric acid (internal standard). The singlet present at 7.80 ppm corresponds to the four aromatic H-atoms of benzene-1,4-dicarboxylic acid in Fig. S3 and Fig. S4, while the three chemically distinguishable H-atoms of 2-aminobenzene-1,4-dicarboxylic acid are featured by three set of signals at 7.62 ppm (doublet), 7.18 ppm (doublet) and 7.111 ppm (double doublet) in Fig. S4 and Fig. S5 Finally, the singlet at 8.39 ppm observed in all spectra corresponds to the C–H atom of formic acid that comes from DMF decomposition.¹

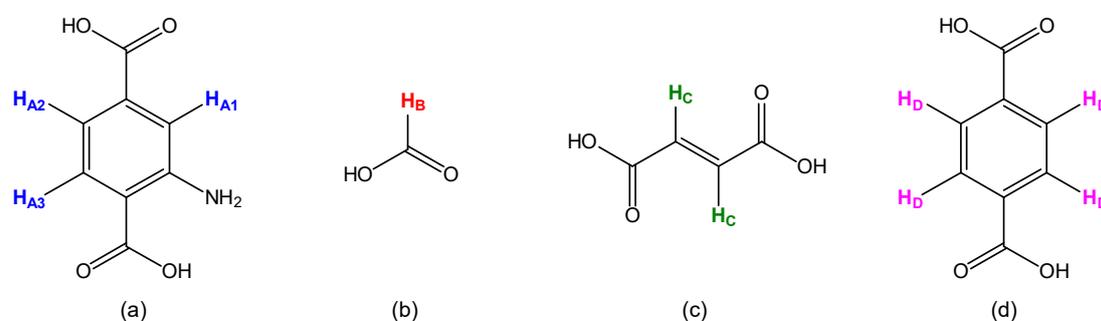


Fig. S2 Proton label assignment for (a) 2-aminobenzene-1,4-dicarboxylic acid, (b) formic acid, (c) fumaric acid and (d) benzene-1,4-dicarboxylic acid for $^1\text{H-NMR}$ spectra.

¹ J. Łuczak, M. Kroczevska, M. Baluk, J. Sowik, P. Mazierski and A. Zaleska-Medynska, *Adv. Colloid Interface Sci.*, 2023, **314**, 102864. DOI: <https://doi.org/10.1016/j.cis.2023.102864>

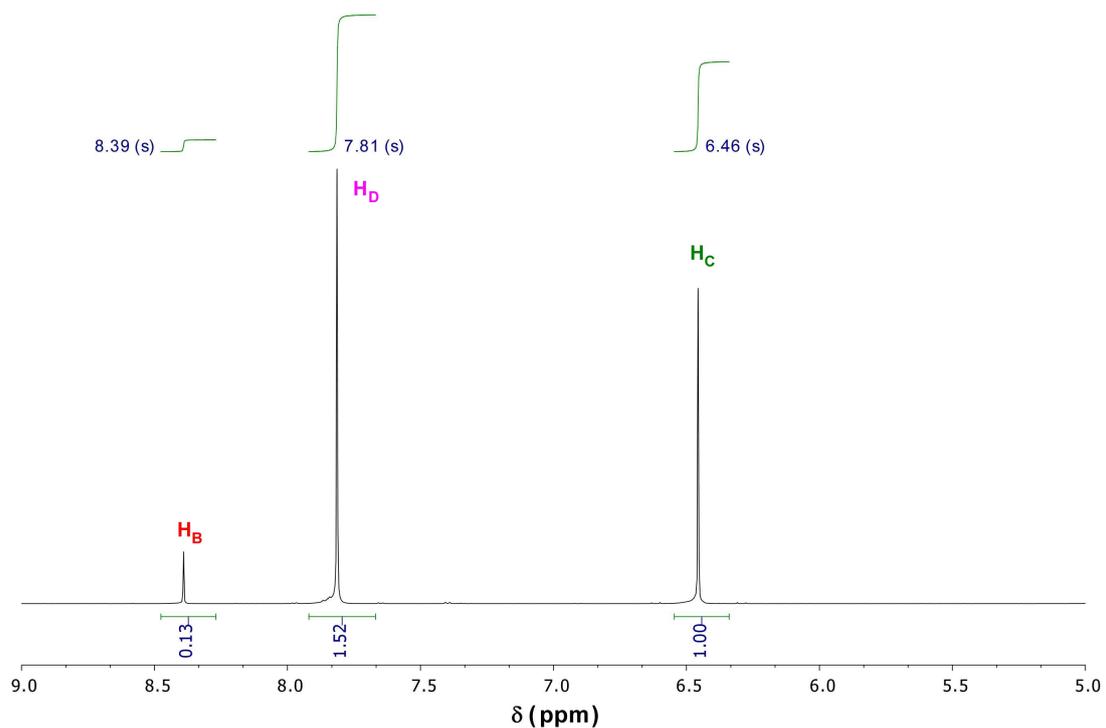


Fig. S3 $^1\text{H-NMR}$ spectrum in D_2O of digested B100.

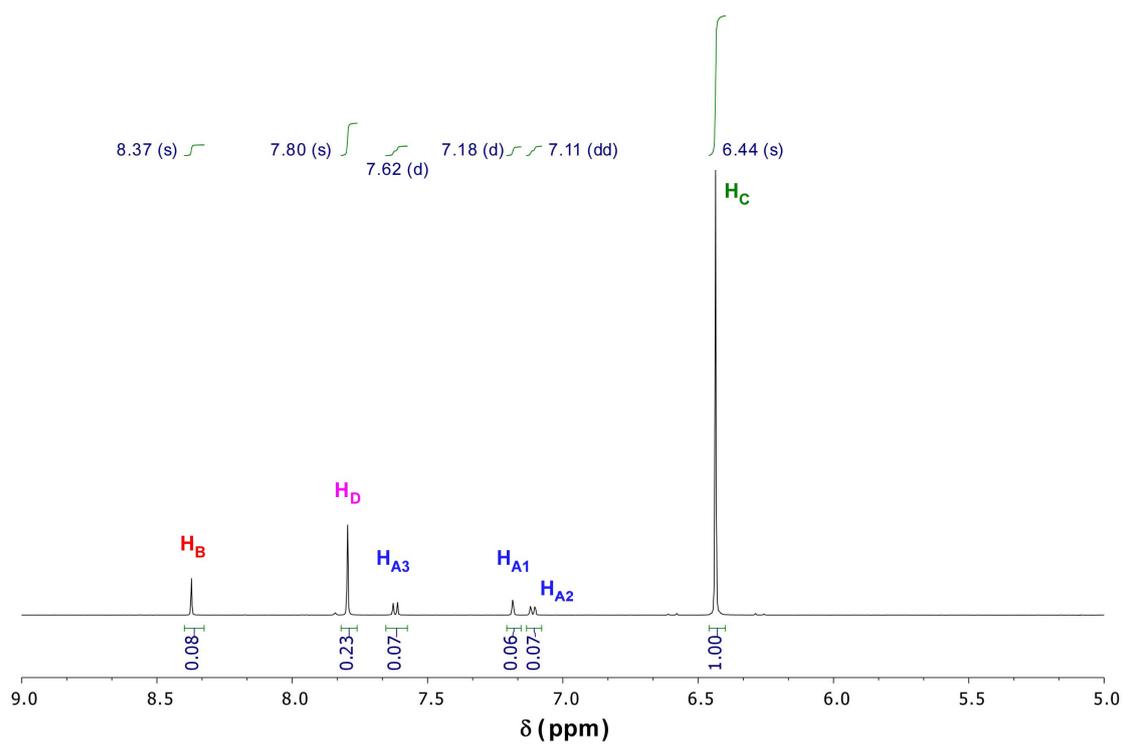


Fig. S4 $^1\text{H-NMR}$ spectrum in D_2O of digested B50A50.

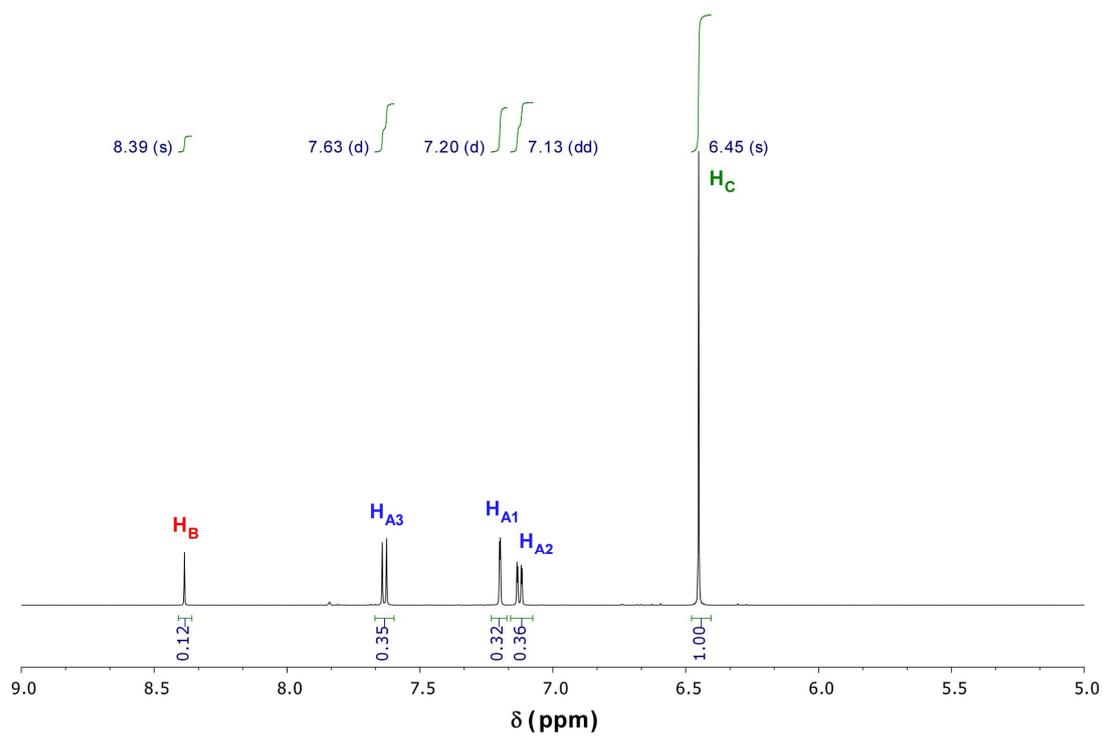


Fig. S5 ¹H-NMR spectrum in D₂O of digested A100.

S4. THERMOGRAVIMETRIC ANALYSIS (TGA)

Fig. S6 shows the thermogravimetric analysis of neat materials performed in synthetic air from 30 °C to 800 °C. The thermograms show three main stages of weight loss. First, solvent molecules contained within the pores are released (30 – 150 °C). Thereafter, at intermediate temperature values (150 – 300 °C), coordinated water molecules that come from the condensation of hydroxide groups and formic acid are released. Finally, the framework decomposition takes place (300 – 500 °C). In the case of B100 sample the framework decomposes exothermically in a single step that starts roughly at 400 °C. The samples containing NH₂BDC ligand (B50A50 and A100) exhibit a mass loss close to 300 °C probably related to the pyrolytic release of the –NH₂ group. This type of decomposition is usually endothermic, however the sensitivity of the DTA signal was not enough to observe a clear peak in this region. Thereafter, around 400 °C the remaining material decomposes again exothermically. In all cases, TiO₂ was formed as final residue, which was identified by PXRD (rutile phase, ICDD PDF No. 00-001-1292, Fig. S7).

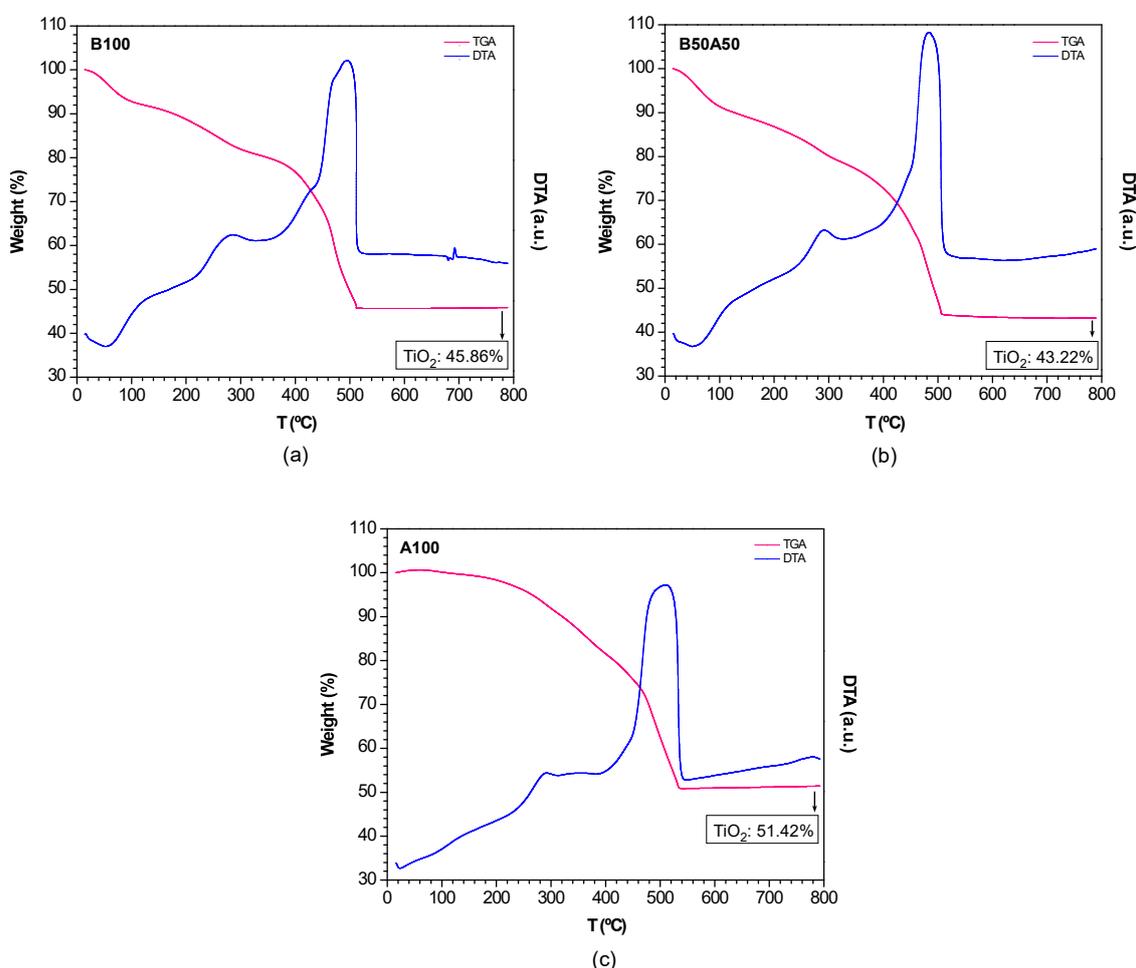


Fig. S6 TGA-DTA curves of (a) B100, (b) B50A50 and (c) A100.

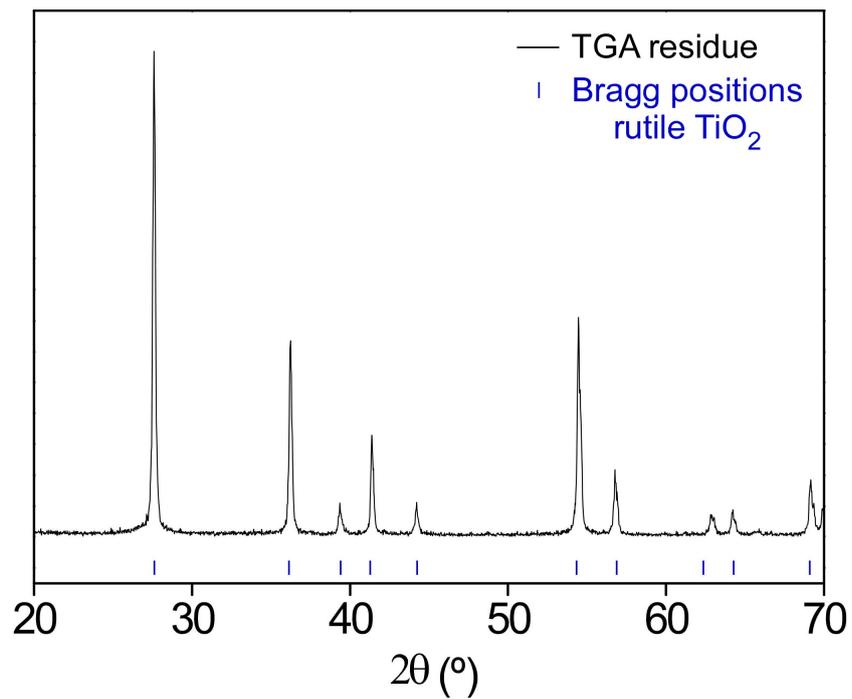


Fig. S7 PXR D of TGA residue of B100 samples, identified as rutile TiO₂ (ICDD PDF No. 00-001-1292).

S5. DEFECTIVE FORMULA ESTIMATION

To determine the formula of the prepared MOGs, $^1\text{H-NMR}$ and TGA measurements were employed. In $^1\text{H-NMR}$ spectra, the amount of dicarboxylic linkers (benzene-1,4-dicarboxylato, BDC and/or 2-amino-benzene-1,4-dicarboxylato, NH_2BDC depending on the sample) and formate (HCOO^- , originating from DMF decomposition during the synthesis procedure) per metal-organic network amount ($\text{mmol/g}_{\text{MOG}}$)^a was determined. This was achieved by using the internal standard amount (fumaric acid) and integration values (see Section S3).

On the other hand, TGA measurements were employed to estimate the quantity of Ti and the molecular weight (MW_{TGA}) of the measured sample, considering that the residue is TiO_2 (see Section S4). The numeric data extracted from this analysis is summarised in Table S2.

Afterwards, taking into account an ideal core of $\text{Ti}_8\text{O}_8(\text{OH})_4$ based on previous studies,² a charge balance was performed to obtain a neutral compound, considering as possible defect compensating ligand water/hydroxide pairs, as extracted from literature concerning ideal MIL-125 MOFs³ (see Table S3).

Finally, the resulting estimated molecular weight ($\text{MW}_{\text{formula}}$) obtained was compared to the one calculated from TGA analysis to validate the formula. It is important to note that this estimation serves as an approximation of the defect formula, being conscious that the material is likely a result of a combination of various defects types within the network. Nevertheless, it enhances our understanding of the nature of the prepared materials.

Table S2 Summary of $^1\text{H-NMR}$ and TGA extracted data for determining an estimated defective formula of prepared MOGs.

Sample	$^1\text{H-NMR}$ analysis			TGA analysis	
	BDC	NH_2BDC ($\text{mmol/g}_{\text{MOG}}$)	HCOO^-	Ti ($\text{mmol/g}_{\text{MOG}}$)	MW_{TGA} ($\text{g}\cdot\text{mol}^{-1}$)
B100	2.39	0	0.82	5.74	1293
B50A50	1.04	0.85	1.11	6.74	1103
A100	0	2.39	0.75	6.44	1243

Table S3 Formula normalization to Ti_8O_8 core and charge balance including water/hydroxide pairs as defect compensating ligand.

Sample	Unit per formula / charge					Total charge	$\text{MW}_{\text{formula}}$ ($\text{g}\cdot\text{mol}^{-1}$)
	$\text{Ti}_8\text{O}_8(\text{OH})_4$	BDC	NH_2BDC	HCOO^-	$\text{H}_2\text{O}/\text{OH}^-$		
B100	1 / +12	3.33 / -6.66	–	1.14 / -1.14	4.20 / -4.20	0	1324
B50A50	1 / +12	1.01 / -2.02	1.16 / -2.32	1.32 / -1.32	6.34 / -6.34	0	1234
A100	1 / +12	–	2.96 / -5.92	0.94 / -0.94	5.14 / -5.14	0	1331

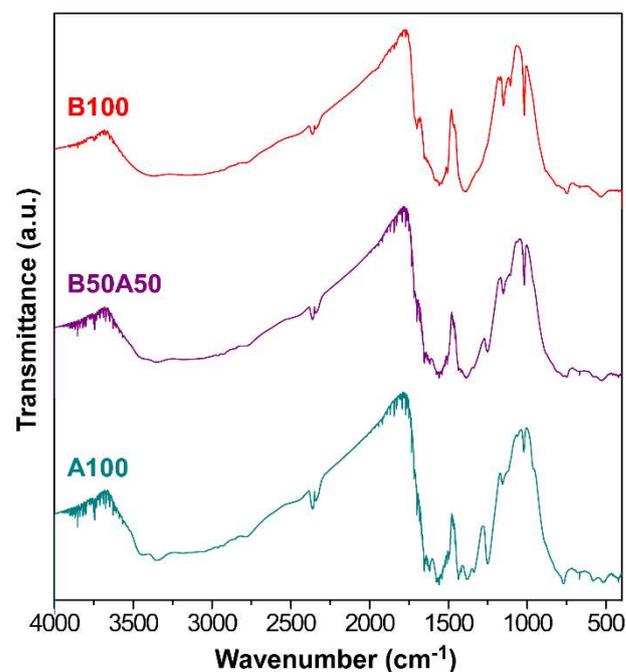
^a The metal-organic network, understood in this case as the dispersed phase within the overall MOG, constitutes the solid component, while the continuous phase is the solvent, which is not considered when calculating specific values. Although the abbreviation MOG is used for simplicity, it is important to note that it specifically refers to the solid portion of the material.

² M. Perfecto-Irigaray, I. Merino-García, J. Albo, G. Beobide, O. Castillo, A. Luque and S. Pérez-Yáñez, *Mater. Today Energy*, 2023, **36**, 101346, DOI: <https://doi.org/10.1016/j.mtener.2023.101346>.

³ L. Pukdeejarhor, S. Wannapaiboon, J. Berger, K. Rodewald, S. Thongratkaew, S. Impeng, J. Warnan, S. Bureekaew and R. A. Fischer, *J. Mater. Chem. A*, 2023, **11**, 9143–9151, DOI: <https://doi.org/10.1039/D2TA09963B>.

S6. FOURIER-TRANSFORM INFRARED SPECTROSCOPY (FTIR)

The infrared spectra of metallogels and the assignment of the main vibration modes are gathered in Fig. S8. The bands shaded in yellow in the table correspond to stretching and deformation vibrations of -NH_2 group, and are, therefore, only observable in B50A50 and A100 samples. The rest of the bands are coincident in the three samples.



Wavenumber (cm ⁻¹)	Band assignment
3460, m	ν_{asym} (NH ₂)
3340, m	ν_{sym} (NH ₂)
1700, sh	ν_{asym} (COO)
1620, m	δ_{ip} (NH ₂)
1560, s	ν (C _{ar} -C)
1500, sh	ν_{ring} (C _{ar} -C _{ar})
1420, sh	ν (C _{ar} -N)
1370, s	ν_{sym} (COO)
1335, sh	δ_{ip} (NH ₂)
1250, s	δ_{oop} (NH ₂)
1020, w	δ (C-H)
760, s	δ_{oop} (C-H) + δ_{oop} (O-C-O)
-500, w	ν (Ti-OCO)

(a)

(b)

Fig. S8 (a) FTIR spectra and (b) band assignments for Ti(IV)/BDC/NH₂BDC-based materials (s: strong, m: medium, w: weak and sh: shoulder signals; *sym.* symmetric, *asym.* antisymmetric, *ip.* in plane, *ring.* ring stretching, *ar.* aromatic, *oop.* out of plane of stretching (ν) or bending (δ) modes).

S7. SCANNING ELECTRON MICROSCOPY (SEM)

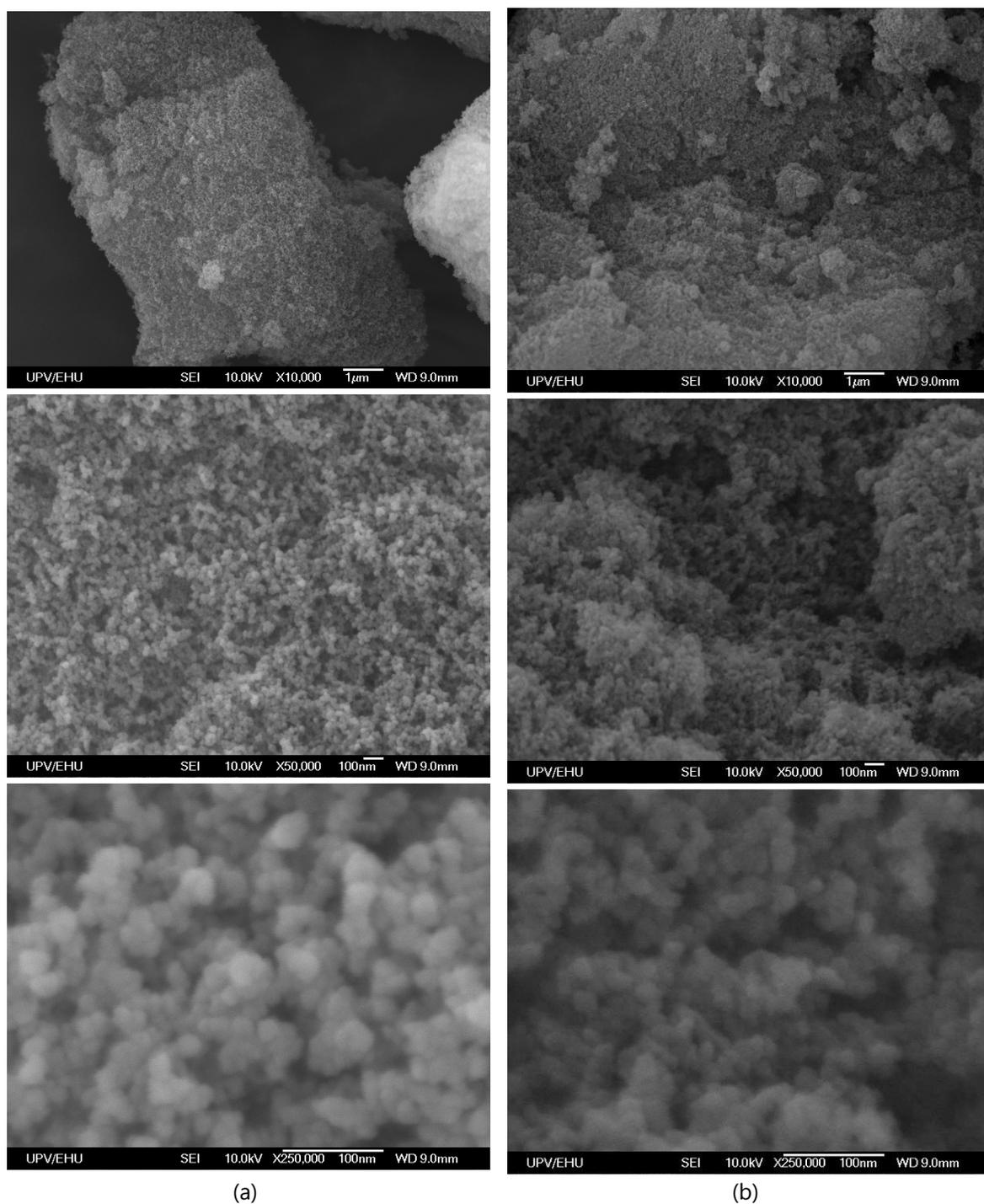


Fig. S9 SEM micrographs taken on (a) B100 and (b) Pt@B100 aerogels at 10 kX (up), 50 kX (middle) and 250 kX (down) magnifications.

S8. SYNCHROTRON X-RAY ABSORPTION SPECTROSCOPY

The k^2 -weighted EXAFS oscillations and corresponding Fourier transform spectra are presented in Fig. S10a-d at both Ti K-edge and Pt L_3 -edge for B100 and Pt@B100, respectively. To determine the local atomic structure, fitting analysis was performed using the obtained data, and the results are reported in Table S4. For the first coordination peak (Fig. S10c), which represents the Ti-O bond lengths, the three Ti-O theoretical coordination paths corresponding to μ -O/ μ -OH and carboxylate groups were combined. Due to the low amplitude of the Ti-Ti coordination peak in B100 and Pt@B100, the second coordination peak was not included in the fitting analysis. At the Pt L_3 -edge of Pt@B100, the first coordination peak (Fig. S10d), has been subjected to fitting analysis. The fitting model considered for this peak includes both the Pt-O coordination and a small contribution from Pt-Pt coordination.

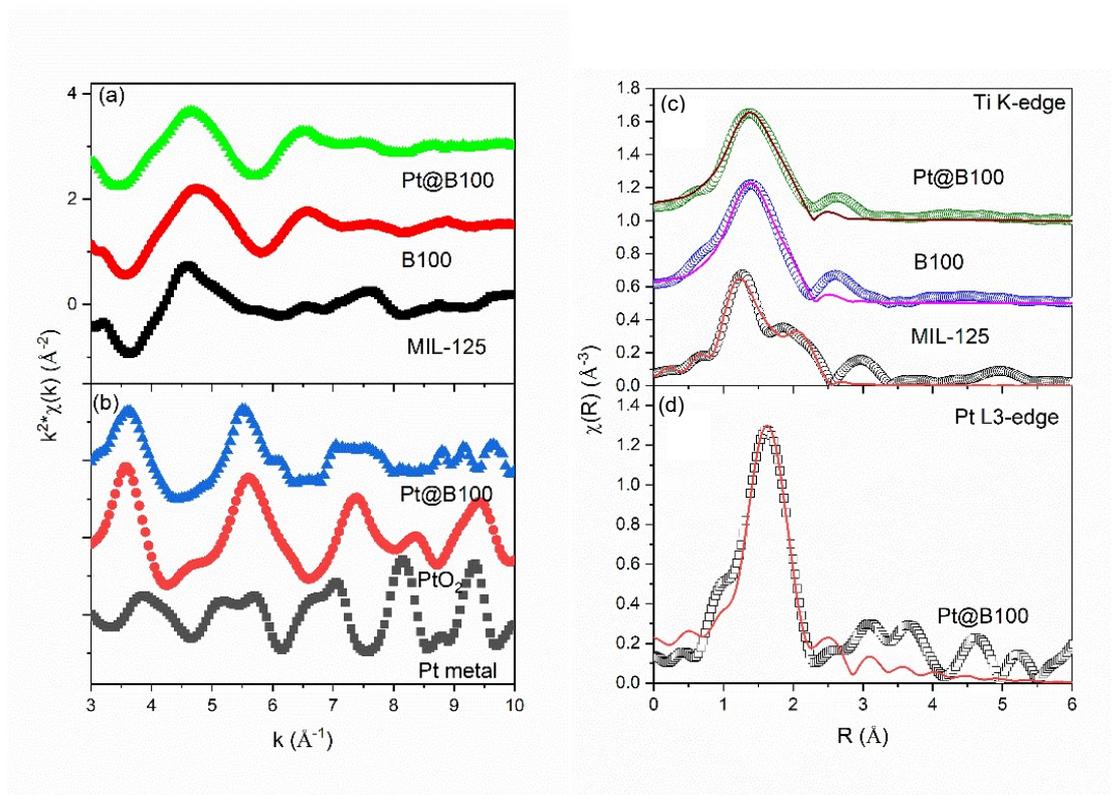


Fig. S10 EXAFS oscillations at (a) Ti K-edge and (b) Pt L_3 -edge. The Fourier transform EXAFS spectra at (c) Ti K-edge and (d) Pt L_3 -edge. The scatter points in c and d represent experimental data and the solid line represents corresponding fitting. The fitting of Fourier transform spectra are shown only for synthesised samples.

Table S4 EXAFS fitting results at Ti K-edge and Pt L₃-edge. *Values are kept constant.

Edge	Sample	Path	R (Å)	N	σ^2 (Å ²)
Ti K-edge	MIL-125	Ti-O	1.83±0.01	6*	0.0135±0.0040
		Ti...Ti	2.59±0.03	1*	0.0071±0.0022
	B100	Ti-O	1.88±0.02	5.90±0.19	0.0136±0.0036
	Pt@B100	Ti-O	1.89±0.02	5.92±0.17	0.0135±0.004
Pt L ₃ -edge	Pt@B100	Pt-O	2.04±0.01	5.28±0.37	0.0079±0.0051
		Pt...Pt	2.65±0.03	0.43±0.17	0.025±0.0079

S9. UV-Vis DIFFUSE REFLECTANCE SPECTROSCOPY (DRS) AND BAND GAP CALCULATIONS

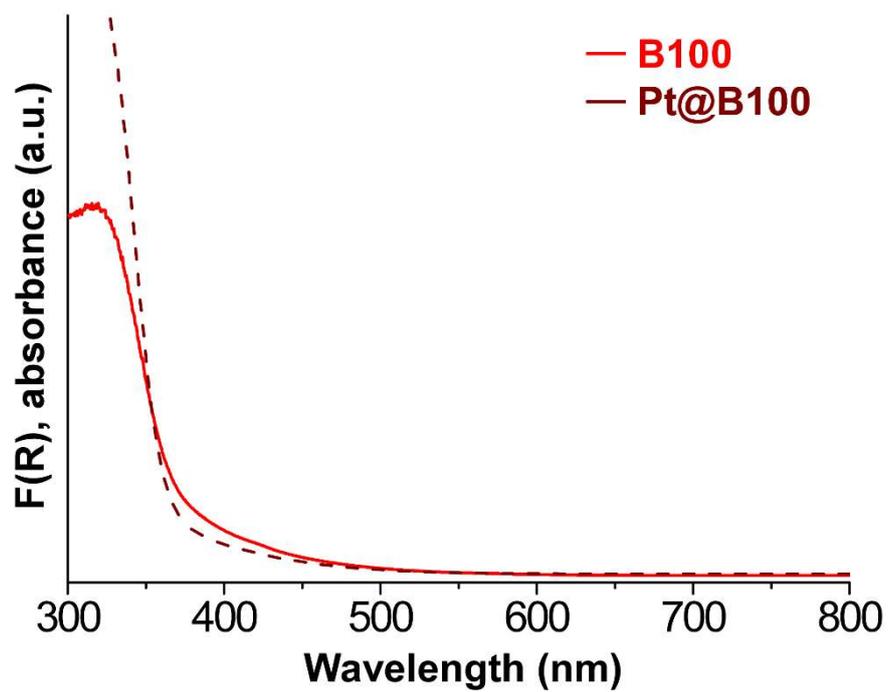


Fig. S11 UV-Vis absorbance spectra derived from Kubelka-Munk function (F(R)) comparison for B100 and Pt@B100.

OPTICAL BAND GAP CALCULATIONS

The optical band gaps of the MOGs were determined from the DRS data using a Tauc plot calculated by fitting the spectra data to Tauc's formula, $(\alpha h\nu)^{1/n} = A(h\nu - E_g)$, where, α is the absorption coefficient, A is a constant, $h\nu$ is the photon energy, and n is a factor related to the type of band gap transition ($n = 0.5$ or 2 for direct or indirect transitions, respectively). The band gap values were obtained from the intersection of the linear fit with the abscissa axis in the $(\alpha h\nu)^{1/n}$ vs $h\nu$ plot (Fig. S12).

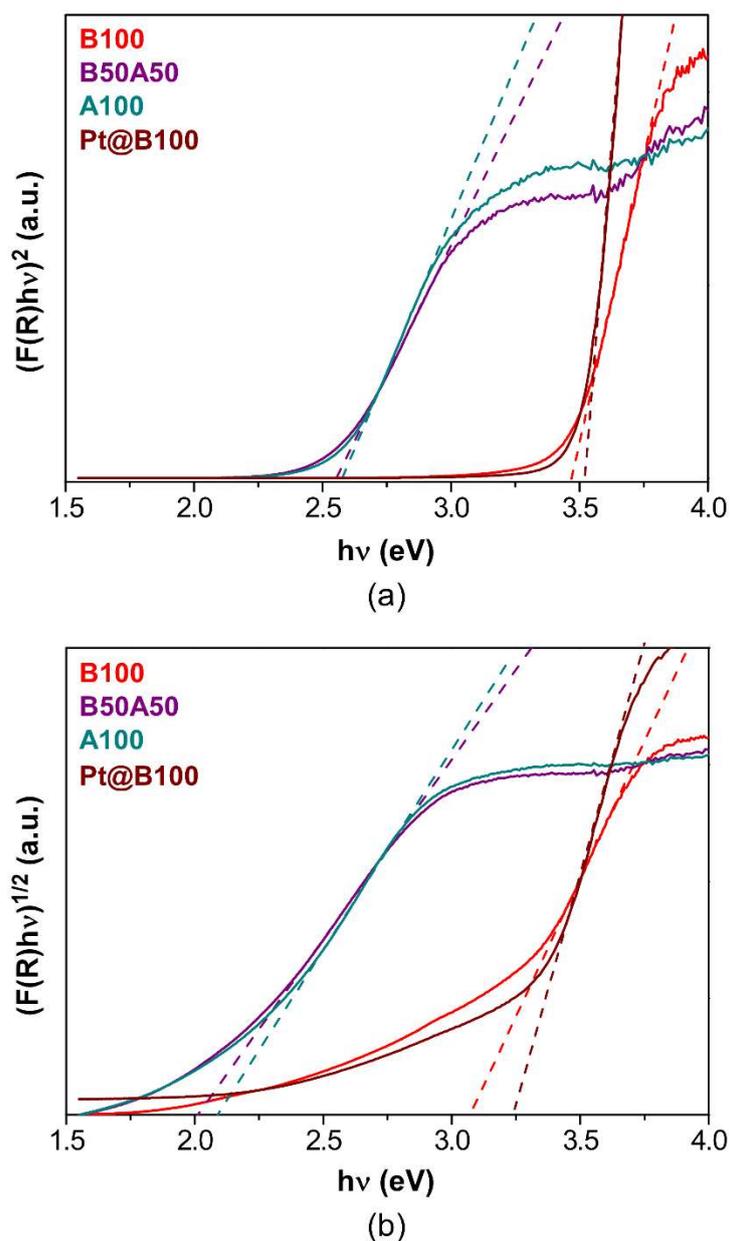
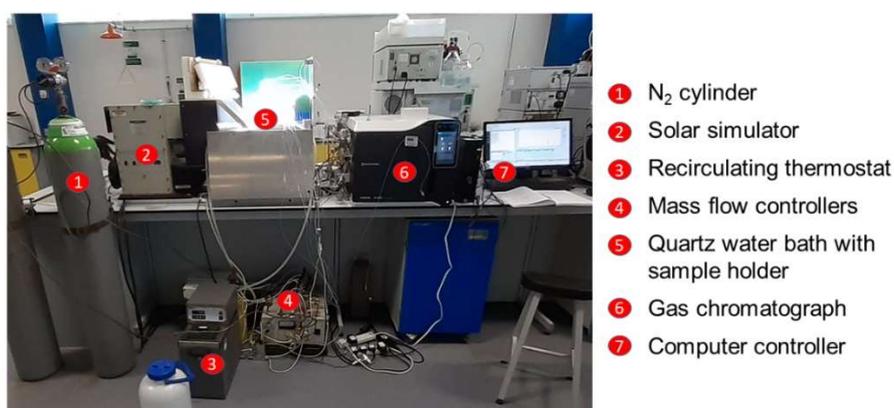


Fig. S12 $(F(R)h\nu)^{1/n}$ vs. $h\nu$ plots for each sample, depicting the linear fit to Tauc equation (dashed lines) for (a) direct with $n = 0.5$ and (b) indirect with $n = 2$ band gaps.

S10. LIGHT-DRIVEN HYDROGEN EVOLUTION REACTION (HER) EXPERIMENTS

Solar-light-driven H₂ production experiments were performed in the set up shown in Fig. S13. Photocatalytic materials (amount of hydrogel to get 5 mg of neat metal-organic network, see Table S5) sealed in a stirred glass vial (Chromacol 10-SV, Fisher) along with 2.0 mL of 0.1 M TEOA aqueous solution are located in a thermostated water bath (25 °C) with continuous stirring and irradiated using a solar light simulator (Thermo Oriel 92194-1000) equipped with an AM 1.5G filter (Newport) with an intensity of 1 sun (100 mW·cm⁻²). The sample headspace was purged with N₂ prior to the measurement (20 mL·min⁻¹, 10 min) and subjected to a constant purge (5 mL·min⁻¹) controlled by a flow controller (Bronkhorst) during the process. H₂ evolution was monitored by a gas chromatograph (Shimadzu Nexis 2030) equipped with a barrier-discharge ionisation detector (BID) and a molecular sieve column (30 m x 0.25 mm x 0.25 μm) using an auto-sampler programmed to inject 2 mL of the selected headspace. The GC was calibrated using calibration gas (2000 ppm H₂, BOC), diluted with N₂ at different ratios using a set of mass flow controllers (Bronkhorst) to provide known concentrations of hydrogen. HER rates were calculated from the measured H₂ concentration in the purge gas and the purge gas flow rate. Cumulative H₂ production was calculated from the H₂ evolution rate and time passed since the previous measurement, assuming a constant H₂ evolution rate between time points.



(a)



(b)

Fig. S13 HER experiments (a) overall set-up and (b) sample position in the quartz water bath exposed to simulated solar light.

Table S5 Amount of water (wt. % of gel's continuous phase) at the prepared MOG-hydrogels and mass of each one needed to obtain *ca.* 5 mg of metal-organic network (MON) for HER measurements.

Sample	H ₂ O wt. %	MOG amount (mg) to get 5 mg of MON
B100	87	39
B50A50	90	48
A100	95	100
Pt@B100	91	56
Pt@B50A50	93	71
Pt@A100	95	100

Fig. S14 shows PXRD pattern of B100 sample after HER experiment conditions with an excess of H₂PtCl₆ as co-catalyst, in which (1 1 1) and (2 0 0) reflections of cubic Pt(0) (ICSD entry: 674735) are observed.

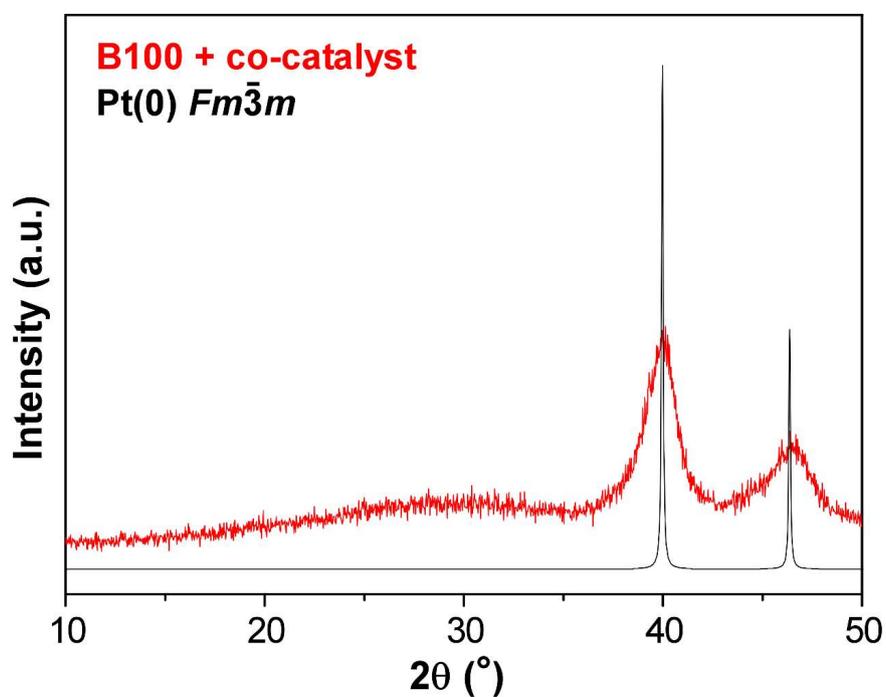


Fig. S14 PXRD of B100 after HER experiment using H₂PtCl₆ as co-catalyst where cubic Pt(0) with 674735-ICSD entry is observed.